



**HAL**  
open science

## Impact of temperature inversions on SST evolution in the South-Eastern Arabian Sea during the pre-summer monsoon season

Fabien Durand, S. R. Shetye, Jérôme Vialard, D. Shankar, S. S. C. Shenoi, Christian Éthé, Gurvan Madec

► **To cite this version:**

Fabien Durand, S. R. Shetye, Jérôme Vialard, D. Shankar, S. S. C. Shenoi, et al.. Impact of temperature inversions on SST evolution in the South-Eastern Arabian Sea during the pre-summer monsoon season. *Geophysical Research Letters*, 2004, 31, pp.L01305. 10.1029/2003GL018906 . hal-00125030

**HAL Id: hal-00125030**

**<https://hal.science/hal-00125030v1>**

Submitted on 11 Feb 2021

**HAL** is a multi-disciplinary open access archive for the deposit and dissemination of scientific research documents, whether they are published or not. The documents may come from teaching and research institutions in France or abroad, or from public or private research centers.

L'archive ouverte pluridisciplinaire **HAL**, est destinée au dépôt et à la diffusion de documents scientifiques de niveau recherche, publiés ou non, émanant des établissements d'enseignement et de recherche français ou étrangers, des laboratoires publics ou privés.

## Impact of temperature inversions on SST evolution in the South-Eastern Arabian Sea during the pre-summer monsoon season

F. Durand,<sup>1</sup> S. R. Shetye,<sup>1</sup> J. Vialard,<sup>2</sup> D. Shankar,<sup>1</sup> S. S. C. Shenoï,<sup>1</sup> C. Ethe,<sup>2</sup> and G. Madec<sup>2</sup>

Received 23 October 2003; accepted 4 December 2003; published 7 January 2004.

[1] Temperature inversions are known to occur in the near-surface ocean regime where salinity stratification is large enough to influence the density field. However, they have not been known as features that alter near-surface processes significantly to influence the sea surface temperature (SST). From the analysis of new observed datasets as well as of state-of-the-art numerical model outputs, this paper shows that heat trapped within a temperature inversion makes significant contribution to warming of the SST in the South-Eastern Arabian Sea during the pre-southwest monsoon season. **INDEX TERMS:** 4572 Oceanography: Physical: Upper ocean processes; 9340 Information Related to Geographic Region: Indian Ocean; 4255 Oceanography: General: Numerical modeling. **Citation:** Durand, F., S. R. Shetye, J. Vialard, D. Shankar, S. S. C. Shenoï, C. Ethe, and G. Madec (2004), Impact of temperature inversions on SST evolution in the South-Eastern Arabian Sea during the pre-summer monsoon season, *Geophys. Res. Lett.*, *31*, L01305, doi:10.1029/2003GL018906.

### 1. Introduction

[2] During the six months prior to onset of the summer monsoon in June, the Lakshadweep Sea presents striking features. During December–March a high in sea level forms in the vicinity of the Lakshadweep Islands [Bruce *et al.*, 1994; Shankar and Shetye, 1997]. The Lakshadweep Sea and its adjoining region become the warmest area of the world ocean, with a so-called mini-warm pool [Joseph, 1990] of SST exceeding 30°C in April and May [Rao and Sivakumar, 1999]. The SST in the tropical Indian Ocean is of prime importance for driving the spatio-temporal evolution of the seasonally reversing winter and summer monsoons [Godfrey *et al.*, 1995]. SST variability in the South-Eastern Arabian Sea (SEAS) is likely to impact the Northern Indian Ocean-summer monsoon coupled system [e.g., Joseph, 1990]. Hence a comprehensive understanding of the evolution of the ocean thermal structure is fundamental to understanding of air-sea coupling in this region. There have been previous attempts to shed light on the processes that drive the evolution of the mini-warm pool of the SEAS. Shenoï *et al.* [1999] provided a unified picture of the surface topography high and the mini-warm pool. It turns out that the SST maximum has its origin in the Bay of Bengal (BB) about 6 months earlier. Downwelling coastal

Kelvin wave packets generated in October in the northern BB enter the SEAS in November–January. They force a current which brings low salinity water from the BB to the SEAS. They propagate poleward along the South-Western Indian coast, radiating downwelling Rossby waves that produce the high in sea level. The downwelling and the inflow of fresher water from BB provide conditions conducive for the formation of the SST high in January. Based on observed climatologies, Rao and Sivakumar [1999] further investigated the heat budget of the mixed layer of the SEAS. They showed that the heat build-up occurring in the mixed layer of the SEAS in the pre-summer monsoon season is primarily driven by the heat flux through the ocean-atmosphere interface. They also provided evidence for the geographic coincidence in the occurrence of the genesis of the monsoon onset atmospheric vortex and the SST maximum. However their diagnostic study clearly suffered from the lack of in-situ data with sufficient coverage. Indeed they concluded that “as the evolution of SST and heat content is fully three-dimensional, an OGCM with good mixed-layer physics can only resolve the mechanisms that produce this mini-warm pool in the Arabian Sea during the pre-summer monsoon season”.

[3] In this paper, we explore the possibility that a near-surface sheet of freshwater may result in temperature inversions and hence in reduction of mixed-layer cooling from below, as described in Vialard and Delecluse [1998a]. Temperature inversion in the surface layer has already been observed in the SEAS during winter from historical bathy thermograph data by Thadathil and Gosh [1992]. At seasonal time scale, an inversion in the upper layer can only be sustained by a sharp haline stratification, the so-called “barrier layer” [e.g., Lukas and Lindstrom, 1991]. In this paper, we analyze new observed datasets as well as state-of-the-art numerical model outputs to address the following questions:

[4] 1) Do the data show a marked inversion and a barrier layer in the SEAS in winter? Is our model consistent with the observed features?

[5] 2) Is the peculiar thermal structure of the SEAS linked with the formation of the SST maximum? The datasets and model are described in section 2. Section 3 presents our main results as regards to the observed and modeled upper-ocean thermal stratification of the SEAS. Section 4 discusses the modeled SST budget in the SEAS.

### 2. The Datasets and Model

[6] We use the weekly 1° × 1° SST product of Reynolds and Smith [1994] to depict the surface pattern of the SEAS warm pool. To gain insight into the three dimensional

<sup>1</sup>Physical Oceanography Division, National Institute of Oceanography, Dona Paula, Goa, India.

<sup>2</sup>Laboratoire d’Océanographie Dynamique et de Climatologie, Université Pierre et Marie Curie, Paris Cedex 05, France.

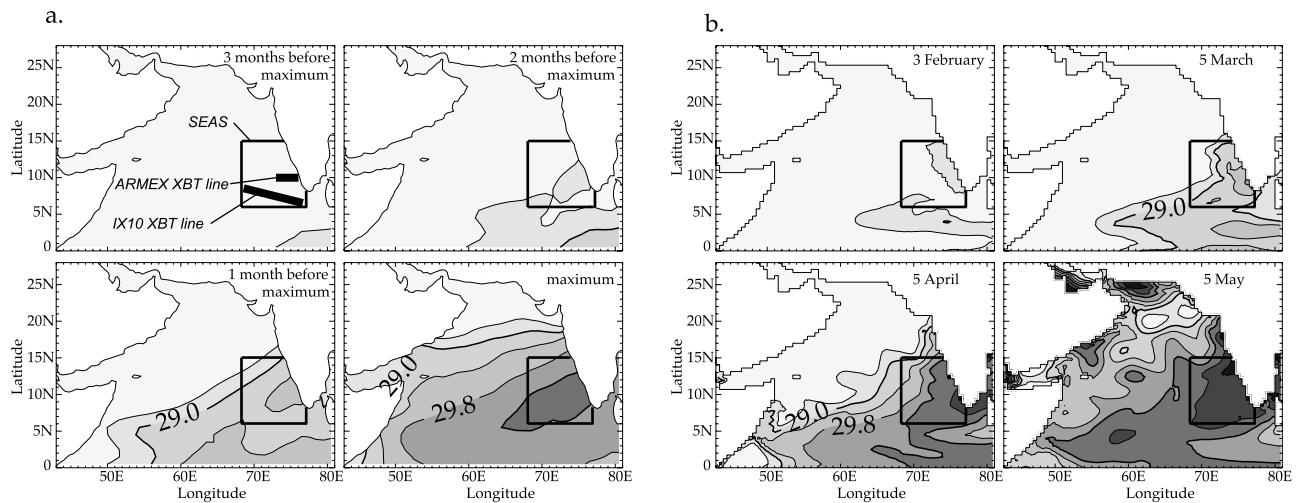


**Figure 1.** Structure of the SST in the Arabian Sea during the spring warming for (a) the composite based on *Reynolds and Smith* [1994] dataset and (b) the model. Iso-contours are every  $0.4^{\circ}\text{C}$ . Superimposed on the plots is the SEAS area shown for further reference. Thick lines on the first plot represent the XBT ship tracks.

thermal structure of the SEAS, we use XBT profiles reported by (D. Shankar, et al., Observational evidence for westward propagation of temperature inversions in the southeastern Arabian Sea, submitted to *Geophys. Res. Lett.*, 2003, hereinafter referred to as Shankar et al., 2003) as well as from WOCE line IX10 available through <http://www.ifremer.fr/sismer>. The Shankar et al., 2003, data are based on a track that goes between Kochi (at  $10^{\circ}\text{N}$  on the southwestern coast of India) and Lakshadweep Islands (situated  $3^{\circ}$  off shore). They were collected within the framework of the Arabian Sea Monsoon EXperiment (ARMEX) program. The second XBT track goes from Aden to Singapore. Figure 1a presents the tracks location. We considered only the profiles falling in the SEAS area, defined by the box ( $68^{\circ}\text{E}; 77^{\circ}\text{E}$ )  $\times$  ( $6^{\circ}\text{N}; 15^{\circ}\text{N}$ ) (Figure 1) since this is the area in which *Shenoi et al.* [1999] identified a peculiar seasonal cycle of SST (see e.g., their Figure 1). The XBT dataset amounts to 262 profiles along the ARMEX line and 1014 profiles along the WOCE IX10 line.

[7] Our model is the OPA OGCM [*Madec et al.*, 1998] applied to the global ocean with  $0.5^{\circ}$  horizontal resolution and 10 m vertical resolution in the upper 120 m. It resolves a state-of-the-art vertical physics based on a prognostic equation for the turbulent kinetic energy [*Blanke and Delecluse*, 1993]. The atmospheric boundary conditions for the OGCM include surface fluxes of momentum, heat and freshwater. The momentum and precipitation fluxes are prescribed, all other fluxes (heat and evaporation) are diagnosed from specified atmospheric variables through bulk formulae. Our forcing strategy consists of simulating the response of the model to the seasonal cycle of the atmospheric fluxes. It is forced by the seasonal climatologies of ERS1-2 wind stress [*Bentamy et al.*, 1996] and CMAP precipitation flux [*Xie and Arkin*, 1996]. The heat and evaporation fluxes are diagnosed from the NCEP reanalysis [*Kalnay et al.*, 1996] air temperature. All fluxes are averaged over the 1993–1999 period. Our version of the model is rather similar to the one used by *Masson et al.* [2003]. Extensive validations of our simulation (not shown) revealed that it successfully reproduces the observed

patterns of monsoon circulation as well as basin-scale thermohaline structure of the Northern Indian Ocean.

[8] The present study focuses on the temperature field of the upper SEAS during the pre-summer monsoon season. Hence it is necessary to validate the model in this regard. To do so, we computed a composite of *Reynolds and Smith* [1994] weekly SST during the 3 month period preceding the time of occurrence of SST maximum in the SEAS area, over the 1982–2002 period (Figure 1a). Hence the SST composites are averaged over 21 years. Consistent with the results of *Shenoi et al.* [1999] for 1989, the composite shows a northward migration of the pool of warm (SST  $> 28.5^{\circ}\text{C}$ ) surface waters in the Arabian Sea, during the three months preceding the SST peak (Figure 1a). The SST peak occurs in late April-early May in most of the individual years (not shown). Again consistent with *Shenoi et al.* [1999], we note that a SST maximum appears in the SEAS region two months before the SST peaks, with a southwest-northeast orientation. The entire southern Arabian Sea warms up during this period, but the warm core in the SEAS remains a well-defined pattern, with SST exceeding by about  $0.8^{\circ}\text{C}$  the values at the same latitude in the western Arabian Sea. A Student's T-test performed over the 1982–2002 period showed that during the 3 months preceding the SST maximum, SST in the SEAS exceeds the SST in the central Arabian Sea (defined by the box  $59^{\circ}\text{E}; 68^{\circ}\text{E} \times 6^{\circ}\text{N}; 15^{\circ}\text{N}$ ) by  $0.65^{\circ}\text{C}$  at the 99% confidence level. It means that this warm core is a robust seasonal feature of the *Reynolds and Smith* [1994] dataset, throughout the period it sampled. Figure 1b presents the corresponding SST sequence in the climatological year of the model. Clearly, there are some inconsistencies between observed and modeled patterns of SST. In particular, the model presents a warm bias of about  $0.4^{\circ}\text{C}$  in the SEAS. We found this bias to be present throughout the year (not shown). The reason for this is not clear. However approximate parameterization of ocean-atmosphere interactions through our bulk formulae is likely to impair the SST of the model, in this area of very warm surface waters. More interestingly, the model reproduces successfully the observed pattern of SST variability, with a

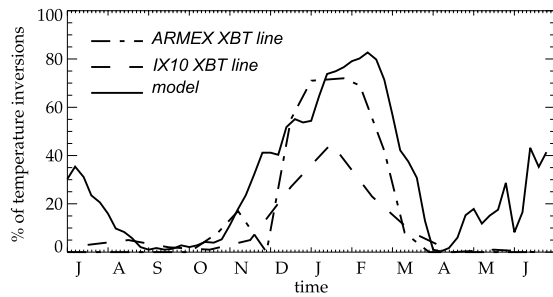


**Figure 2.** Percentage of temperature profiles presenting an inversion observed along IX10 XBT line (dashed line), observed along ARME XBT line (dash-dots, from Shankar *et al.* [2003]) and simulated by the model over the SEAS area (continuous line).

northward progression of the zone of warm ( $SST > 28.5^{\circ}\text{C}$ ) waters from February to March. In the SEAS, the model is in reasonable agreement with the observed feature of Figure 1a: the SST maximum appears along the southwestern coast of India and spreads southwestward throughout the SEAS from early March to early May. In the next section, we investigate the thermohaline structure underlying this pool of warm surface water.

### 3. Temperature Inversion and Upper-Ocean Stratification in the South-Eastern Arabian Sea

[9] Similar to Thadathil and Gosh [1992], we term as inversion a profile where the subsurface temperature exceeds SST by at least  $0.2^{\circ}\text{C}$  at some depth. Both XBT lines exhibit a well defined period of occurrence of inversions in the SEAS, starting in November, peaking by mid-January and disappearing in late March (Figure 2). However, one can note a discrepancy between the two observations sets as regards to the frequency of occurrence of the inversion. Indeed in January for example, 70% of ARME XBTs show an inversion, versus only 40% of IX10 XBTs. It is very likely that the reason for this is linked with the different period sampled in the two datasets. Indeed all ARME XBTs were launched between mid-2002 and mid-2003 [Shankar *et al.*, 2003]. On the contrary, IX10 profiles sample the entire 1988–2002 period. The higher likelihood of temperature inversion in ARME dataset may be related to the particular thermal structure of the SEAS during winter 2002–2003. The model is consistent with the observed timing of the inversion in winter, with an appearance in November and a disappearance in March (Figure 2). However, it slightly overestimates the duration of the inversion-prone period. The maximum frequency of the inversion in the model also appears in mid-February, i.e., 1 month later than in the observations. The frequency of occurrence of modeled inversion peaks at 80%, which is fairly comparable with the observed values along the XBT lines.

[10] Near-surface temperature inversion can only be sustained at seasonal time scales by a sharp haline stratification of the warm layer, i.e. a barrier layer. Rao and Sivakumar [2003] made an attempt to document the barrier layer thickness at basin scale throughout the Northern Indian Ocean. Our model exhibits a thick ( $>20\text{ m}$ ) barrier layer

in the SEAS from early January to mid April, i.e., throughout the period of occurrence of the temperature inversion (Figure 3a). We defined the barrier layer thickness applying the same criterion as Rao and Sivakumar [2003] to the model outputs. The available salinity subsurface data did not allow Rao and Sivakumar [2003] to go into details at the scale of our area of interest. Hence the comparison between their observed features and our model outputs should be considered with great care. However one can note a fairly good agreement of the model with their results in terms of timing of the appearance, peak and disappearance of the barrier layer in the SEAS, as well as thickness of the barrier layer. Interestingly, the pre-monsoonal increase in SST over the SEAS starts when the modeled barrier layer reaches its mature phase, in mid-February (Figure 3a). The barrier layer is known to inhibit the cooling of surface water by lessening the dynamical exchanges between surface and thermocline [Vialard and Delecluse, 1998b]. In the presence of a marked temperature inversion in the barrier layer, Smyth *et al.* [1996] showed that the vertical processes can even warm up the surface layer, through turbulent entrainment. This is suggestive of the following scenario for the SEAS warm pool: a thick barrier layer arises in January–February, sustaining a well-marked inversion. This inversion in turn contributes to raising significantly the SST, by suppressing the entrainment cooling at the bottom of the mixed layer or even by warming the mixed layer. This is what we assess in the following section.

### 4. Heat Budget of the South-Eastern Arabian Sea

[11] We inferred a quantitative heat budget of the SEAS with our OGCM, following the methodology defined by Vialard and Delecluse [1998a]. Briefly, it consists of averaging the model temperature tendency terms over the time-varying mixed layer thickness, distinguishing between

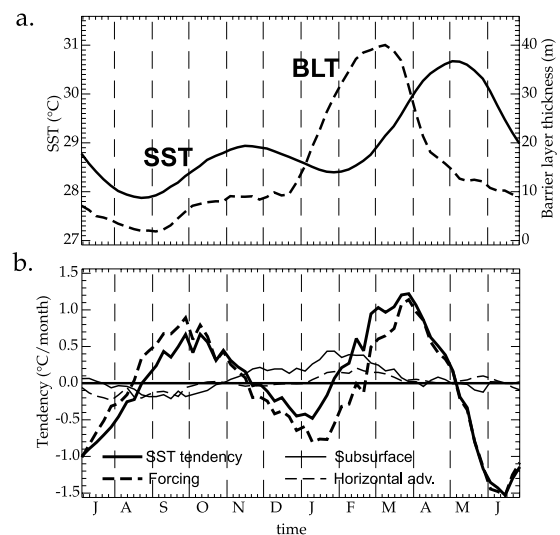


**Figure 3.** Time evolution of the model SST (continuous line) and barrier layer thickness (dashed line) in the SEAS area (a). Corresponding time evolution of SST tendencies in the model, in  $^{\circ}\text{C}/\text{month}$  (b). Effect of the atmospheric forcing (thick dashed line). Horizontal advection (thin dashed line). Subsurface tendency (thin continuous line). Total SST tendency (thick continuous line).

the effects of forcing, subsurface processes (vertical advection, mixing and entrainment), and horizontal advection. The time evolution of the various terms averaged over the SEAS is presented in Figure 3b. Overall, we can see that at annual timescale the modeled variability of SST is primarily driven by the atmospheric forcing. The effect of horizontal advection remains weak throughout the year. This is consistent with the conclusions drawn by *Rao and Sivakumar* [1999] from observations-based heat budget during the December–April period. *Rao and Sivakumar* [1999] could not assess the impact of vertical processes on SST in the SEAS. However, a closer examination of the modeled heat budget during the pre-summer monsoon season reveals that the cooling effect of the vertical processes is suppressed during the November–May period, i.e. during the time when the thick barrier layer is present in our simulation. More interestingly, the vertical processes warm significantly the mixed layer during the time of occurrence of the inversion (early December to end of February), with values reaching +0.4K/month from mid-January to mid-February. At the end of January, the warming effect of the vertical processes starts dominating the cooling effect of the atmospheric forcing. This results in a net warming of the mixed layer. This warming starts one month earlier than when the forcing term becomes positive. This is likely to explain the one month phase lead of the seasonal cycle of SST in the SEAS as compared to the surrounding region, evidenced by *Shenoi et al.* [1999]. Over the November–March period, the integrated subsurface tendency warms the mixed layer by 1.1°C, whereas the forcing cools it by 0.3°C.

[12] In the light of our analysis, we suggest a unified picture of the climatic peculiarities of the SEAS during the pre-summer monsoon season. The high in sea level appears in December and is immediately followed by a thickening of the barrier layer. This allows sustaining a marked temperature inversion, which in turn warms up the mixed layer through vertical processes. It results in a rise of SST starting one month before atmospheric forcing term becomes positive. Hence it appears that the temperature inversion in the SEAS is of crucial importance in explaining the early rise and high peak value of SST in this area. At this stage, the sharp haline stratification of the upper SEAS appears as a key-factor of the whole picture we display. The formation mechanisms of the barrier layer remain to be identified. To shed light on this issue, a salt budget of the SEAS is required. This will be explored in a future study. Also, previous studies noted that SST peaking earlier and higher in the SEAS than in the surrounding region is likely to markedly impact the behavior of the northern Indian ocean – summer monsoon coupled system. The atmospheric response to the SST maximum remains to be clarified in order to be able to monitor the seasonal picture of the summer monsoon onset, as well as its interannual variability.

[13] **Acknowledgments.** SRS, DS and SSCS thank DST and DOD, New Delhi for funding support. We are thankful to SISMER (Ifremer,

France) for having made available the IX10 XBT data. FD was funded by a Lavoisier Grant from French Ministry of Foreign Affairs. SAXO, the plotting software developed by S. Masson, was very helpful. The OGCM experiments were carried out on the NEC SX-5 of the Institut de Recherche et de Développement en Informatique Scientifique (IDRIS). This is NIO Contribution 3856.

## References

- Bentamy, A., Y. Quilfen, F. Gohin, N. Grima, M. Lenaour, and J. Servain (1996), Determination and validation of average wind fields from ERS-1 scatterometer measurements, *Global Atmos. Ocean Syst.*, *4*, 1–29.
- Blanke, B., and P. Delecluse (1993), Variability of the tropical Atlantic Ocean simulated by a general circulation model with two different mixed layer physics, *J. Phys. Oceanogr.*, *23*, 1363–1388.
- Bruce, J. G., D. R. Johnson, and J. C. Kindle (1994), Evidence for eddy formation in the eastern Arabian Sea during the northeast monsoon, *J. Geophys. Res.*, *99*(C4), 7651–7664.
- Godfrey, J. S., A. Alexiou, A. G. Ilahude, D. M. Legler, M. E. Luther, J. P. McCreary, G. A. Meyers, K. Mizuno, R. R. Rao, S. R. Shetye, J. H. Toole, and S. Wacongne (1995), The role of the Indian Ocean in the Global Climate System: Recommendations regarding the Global Ocean Observing System. Report of the Ocean Observing System Development Panel, Texas A&M Univ., College Station, TX, USA.
- Joseph, P. V. (1990), Warm Pool over the Indian Ocean and Monsoon Onset, *Tropical Ocean-Atmos. News Lett.*, *53*, 1–5.
- Kalnay, E., et al. (1996), The NCEP/NCAR 40–Year Reanalysis Project, *Bull. Am. Meteorol. Soc.*, *77*, 437–471.
- Lukas, R., and E. Lindstrom (1991), The mixed layer of the western equatorial Pacific Ocean, *J. Geophys. Res.*, *96*(Supplement), 3343–3358.
- Madec, G., P. Delecluse, M. Imbard, and C. Levy (1998), OPA 8.1 Ocean General Circulation Model reference manual. Note du Pole de modélisation, Institut Pierre-Simon Laplace (IPSL), France, N°11, 91 pp.
- Masson, S., J.-P. Boulanger, C. Menkes, P. Delecluse, and T. Yamagata (1997), Impact of salinity on the 1997 Indian Ocean dipole event in a numerical experiment, *J. Geophys. Res.*, in press.
- Rao, R. R., and R. Sivakumar (1999), On the possible mechanisms of the evolution of a mini-warm pool during the pre-summer monsoon season and the onset vortex in the southeastern Arabian Sea, *Q. J. R. Meteorol. Soc.*, *125*, 787–809.
- Rao, R. R., and R. Sivakumar (2003), Seasonal variability of sea surface salinity and salt budget of the mixed layer of the north Indian Ocean, *J. Geophys. Res.*, *108*(C1), 3009, doi:10.1029/2001JC000907.
- Reynolds, D., and T. Smith (1994), Improved global sea surface temperature analyses using optimum interpolation, *J. Clim.*, *7*, 929–948.
- Shankar, D., and S. R. Shetye (1997), On the dynamics of the Lakshadweep high and low in the southeastern Arabian Sea, *J. Geophys. Res.*, *102*(C6), 12,551–12,562.
- Shenoi, S. S. C., D. Shankar, and S. R. Shetye (1999), On the sea surface temperature high in the Lakshadweep Sea before the onset of the southwest monsoon, *J. Geophys. Res.*, *104*(C7), 15,703–15,712.
- Smyth, W. D., D. Hebert, and J. N. Moum (1996), Local ocean response to a multiphase westerly wind burst, 2, Thermal and freshwater responses, *J. Geophys. Res.*, *101*, 22,513–22,534.
- Thadathil, P., and A. K. Gosh (1992), Surface Layer Temperature Inversion in the Arabian Sea during Winter, *J. Oceanogr.*, *48*, 293–304.
- Vialard, J., and P. Delecluse (1998a), An OGCM study for the TOGA decade. Part I: Role of salinity in the physics of the western Pacific fresh pool, *J. Phys. Oceanogr.*, *28*, 1071–1088.
- Vialard, J., and P. Delecluse (1998b), An OGCM study for the TOGA decade. Part II: Barrier layer formation and variability, *J. Phys. Oceanogr.*, *28*, 1089–1106.
- Xie, P., and P. Arkin (1996), Analyses of global monthly precipitation using gauge observations, satellite estimates, and numerical model predictions, *J. Clim.*, *9*, 840–858.

F. Durand, D. Shankar, S. S. C. Shenoi, and S. R. Shetye, Physical Oceanography Division, National Institute of Oceanography, Dona Paula, Goa 403004, India. (fdurand@darya.nio.org)

C. Ethe, G. Madec, and J. Vialard, Laboratoire d’Océanographie Dynamique et de Climatologie, Université Pierre et Marie Curie, 4 Place Jussieu, 75252 Paris Cedex 05, France.